Atomic description and velocity effects for surface-plasmon neutralization rates in $He^+(1s)$/Al systems

F. A. Gutierrez[1,*] and H. Jouin[2]
[1]*Departamento de Física, Universidad de Concepción, Casilla 4009, Concepción, Chile*
[2]*CELIA (UMR 5107 du CNRS), Université Bordeaux I, 351 Cours de la Libération, 33405 Talence Cedex, France*
(Received 20 February 2003; published 24 July 2003)

In this work we study the effects of both atomic description and ion velocity on the surface-plasmon mediated neutralization rates for low energy $He^+(1s)$ ions interacting with Al surfaces. The transition rates appear to have a weak velocity dependence for ion velocities below 0.5 a.u. It is also shown that differences in the atomic description of the final neutral helium atoms are responsible for the strong discrepancies between recently published surface plasmon transition rates and earlier multielectron Auger rates. The relevance of the surface collective response during the ion neutralization is illustrated for intermediate and large ion-surface distances. For the case of grazing incidence, we analyze the velocity effects for the corresponding angular distributions of the final neutral He atoms. Earlier calculations had been performed within the fixed ion approximation. We find that although both the collective neutralization rates and the neutralized fractions depend very weakly on the parallel velocity, its effects on the angular distributions are clearly noticeable.

DOI: 10.1103/PhysRevA.68.012903 PACS number(s): 79.20.Rf

I. INTRODUCTION

In recent years the relevance of the (one-electron) resonance tunneling mode [1] and the (two-electrons) Auger capture [2] for ion neutralization at metallic surfaces has been diminished by the presently better comprehension about the important role played by the collective response of the metal to the external perturbation produced by the incoming ion. This collective response, which is supported by the long-range correlations between the metal electrons, gives rise to multielectron modes, such as the surface-plasmon mode of ion neutralization [3], in which one metal electron in the conduction band emits a surface-plasmon while getting captured into a low-lying atomic level (essentially the ground state for monocharged ions). The relevance of the pure surface plasmon (PSP) mode was illustrated by further work [4] performed with a Hamiltonian approach with the conclusion that the collective neutralization rates could be larger than the Auger rates at intermediate and large ion-surface distances. A similar qualitative conclusion was obtained in Ref. [5] through the evaluation of multielectron Auger (MEA) neutralization rates, which include simultaneously, by application of a dielectric response formalism, the contributions from the usual two-electron Auger capture and those related to surface-plasmon-induced transitions. These theoretical findings seem to be qualitatively ratified by a bunch of recent experimental reports on electron emission spectra, some of which indicate that surface-plasmon modes should dominate the neutralization behavior in most cases where they are energetically allowed [6,7].

We note that this collective surface mode of neutralization—also termed potential surface-plasmon emission [7]—exists independent of the state of motion of the projectile, as long as the total energy of the system is conserved in the process, so that the neutralization can occur even if the ion is at rest. It contrasts with the usual scenario for *kinetic surface-plasmon excitation*, which is known to be present only for projectile ions with velocities above a certain threshold velocity v_{thr} [6]. In fact, Mills [8] has found that $v_{thr}=\omega_{sp}/k_F$ with ω_{sp} the frequency of surface plasmons and k_F the Fermi wave vector for the metal. For Al one has $\omega_{sp}=0.39$ and $k_F=0.93$ so that $v_{thr}=0.42$ a.u. For bulk plasmons the threshold velocity for emission is larger than 1 a.u. [7]. The most recent experimental reports in the literature [6] indicate that both kinetic and potential surface-plasmon emission seem to contribute importantly to the structure of electron emission spectra induced by ion-surface collisions.

On the other hand, the recent experimental reports [9] for neutralized fractions and angular distributions of low-energy neutralized helium atoms, after grazing incidence interaction of He^+ ions with metallic surfaces, provide valuable information to test existing theoretical transition rates (together with their related models) for the different processes, which can contribute to electron capture at metal surfaces by the projectile ion. A nice feature of these experiments is that the incoming ion has velocities well below v_{thr} so that the above-mentioned kinetic surface plasmon emission process does not play any role here. In particular, the He^+/Al(111) system has been studied with some detail [9,10].

In order to test the relevance of collective surface modes during the electron capture we have recently [11] evaluated PSP neutralization rates for the He^+/Al system and analyzed their contribution to the angular distribution of neutral helium after neutralization of He^+ on Al surfaces under grazing incidence conditions. Angular distributions for the above-mentioned MEA modes [5] were also obtained there by application of the more recent rates reported in Refs. [12,13]. We found the following [11].

(1) Our PSP rates are much larger than the MEA rates at

*Corresponding author. FAX: (56) (41) 224520; email: fgutierr@udec.cl

intermediate and large distances contrary to the expectations, since in principle the PSP contribution is supposed to be contained in the MEA rates. At that time it was not clear to us which was the source of the disagreement so that this point was left unsolved.

(2) The angular distribution for the neutralized He atoms obtained with the PSP rates was consistent in peak's position and angular range with the experimental data although the contribution of the collective process alone is not enough to reproduce the height of the normalized experimental angular distribution.

(3) The angular distribution related to the MEA mode appeared to be appreciably more underestimated than the PSP angular distribution at small angles and clearly overestimated at large angles as compared to the experimental curve. The underestimation at small angles is related to the extremely low values of the MEA rates at large ion-surface distances, a situation already noted in Ref. [10], although in that work the use of the very crude classical image potential might be the main responsible for the large disagreement between theory and experiments. The overestimation of the MEA angular distribution at large angles can be traced back to a possible overestimation of the MEA rates at short ion-surface distances.

In the above calculations the transition rates for the PSP mode were obtained within the fixed ion approximation (FIA), the same as the MEA rates [5,12,13]. To obtain the angular distributions we assumed [11] that the FIA was a reasonable first approximation for the rates, although no proof was given about the smallness of the velocity effects. Therefore, in principle, there is a little unconsistency in that procedure since evaluations of angular distributions—where the rates are crucial ingredients—assume that the ion is moving. This unconsistency is removed here by the calculation of velocity-dependent PSP transition rates and by their application to obtain angular distributions, which can be compared consistently with the experimental results. Although we report results of PSP rates for the range $v \lesssim 1.0$ a.u. our primary interest is in the range of $v \lesssim 0.4$ a.u., which corresponds to the velocity regime where kinetic plasmon emission cannot be present. Furthermore, the choice of low velocities will allow us to compare our calculated angular distributions with the experimental angular distributions of Hecht, Winter, and Borisov [10] for neutral helium, which were obtained for $v = 0.14$ a.u. We shall see that consideration of ion's velocity affects the transition rates for the PSP mode in two ways: (i) the disappearance of the short-distance FIA threshold below which the PSP rates vanish, and (ii) a small decrease of the PSP rates for certain ranges of ion-surface distance.

In Ref. [11] the main concern was the evaluation of angular distributions, which could be compared with experimental results so that a detailed analysis of the description of the final bound atomic state, which is produced by the neutralization process, was not given there. We present such analysis here with the conclusion that the above-mentioned discrepancies between the PSP and the MEA rates at intermediate and large distances are related to the different representations for the final atomic wave function considered in the two different approaches.

In Sec. II we summarize both the theory for surface-plasmon transition rates (velocity effects included) and the procedure to obtain the corresponding angular distributions. The results and all the relevant discussions appear in Sec. III. In particular, we present there a simple qualitative analysis to illustrate why, in those cases where potential emission of a surface-plasmon is energetically allowed, the transition rate for the collective process can be expected to be larger than the (two-electron) Auger rate during the ion-surface encounter, especially at large distances. The main conclusions are summarized in Sec. IV. Atomic units are used throughout this paper unless otherwise stated.

II. THEORY

A. Surface-plasmon neutralization rates

The dependence of the collective neutralization rates on the velocity v of the ion will be taken into account by performing all the calculations in the "ion system," in which the ion is at rest while the solid moves with velocity $(-v)$. In this way the velocity effects will be totally included in the wave function for the initial (metal) electron state ($|\Phi^{(i)}_{\mathbf{k}-\mathbf{v}}\rangle$) with momentum $k-v$. The usual Galilean transformation [14,15]

$$|\Phi^{(i)}_{\mathbf{k}-\mathbf{v}}\rangle = e^{i[(mv^2/2)-E]t} e^{-i\mathbf{v}\cdot\mathbf{r}} |\Phi^{(i)}_{\mathbf{k}}\rangle \tag{1}$$

relates the initial electron state $|\Phi^{(i)}_{\mathbf{k}-\mathbf{v}}\rangle$ in the ion's reference frame with the initial electron state $|\Phi^{(i)}_{\mathbf{k}}\rangle$ in the solid's reference frame. In this work we shall consider the approximation $v = v_{\parallel}$. This is a very reasonable approximation since, for the case of low-energy grazing collisions where the energies are of a few keV and the angles of incidence are around 1°, the effects of the perpendicular velocity should be smaller than 1%.

Within the orthogonalized first Born approximation the transition rate for the pure surface-plasmon mode of ion neutralization is given by [3,11]

$$\Gamma_{\mathrm{PSP}} = 2\pi \sum_{\mathbf{k},\mathbf{q}<\mathbf{q}_c} |\langle \Phi^{(f)}_n, \mathbf{q}|H_{int}|\Phi^{(i)}_{\mathbf{k}-\mathbf{v}}\rangle|^2 \delta(\varepsilon_i - \varepsilon_f), \tag{2}$$

where $\varepsilon_i = \frac{1}{2}(\mathbf{k}-\mathbf{v})^2$ is the energy of the initial state $|\Phi^{(i)}_{\mathbf{k}-\mathbf{v}}\rangle$, which is orthogonal to $|\Phi^{(f)}_n, \mathbf{q}\rangle$ and which represents an electron with momentum $\mathbf{k}-\mathbf{v}$ in the conduction band. The energy $\varepsilon_f(s,q)$ of the final state $|\Phi^{(f)}_n, \mathbf{q}\rangle$, for an electron lying on an atomic state labeled "n" and for a plasmon of wave vector $\mathbf{q}(q,\varphi_q)$ and energy $\omega_s(q)$, is (with respect to the bottom of the conduction band)

$$\varepsilon_f(s,q) = V_0 - E_n(s) + \omega_s(q), \tag{3}$$

with $V_0 = E_F + W$ the depth of the conduction band (E_F being the Fermi energy and W the corresponding work function) and $E_n(s)$ the bound energy of the final atomic state, which is a function of the ion-image plane distance s due to the atom-surface interaction. As is well known [16] q_c is the

momentum cutoff beyond which the plasmon is strongly (Landau) damped. From Eqs. (1) and (2) one can see that, since the additional time-dependent phase factor will disappear when taking the square modulus of the matrix elements, the only relevant difference between the velocity-dependent matrix elements and the FIA matrix elements is the factor $e^{-i\mathbf{v}\cdot\mathbf{r}}$. Therefore, the calculations of the velocity-dependent matrix elements will follow similar lines as those performed within the FIA [11].

The electron-surface plasmon coupling [3,4,11] is

$$H_{int}=\sqrt{\frac{\pi\omega_s(q)}{q\mathcal{A}}}\,e^{-i\mathbf{q}\cdot\boldsymbol{\rho}}e^{-q|z+s|},\quad q\leqslant q_c \tag{4}$$

with $\mathcal{A}$ the elementary area, (ρ,φ,z) the electronic cylindrical coordinates ($\boldsymbol{\rho}$ and z being parallel and perpendicular to the surface plane, respectively) and with the origin of electronic coordinates located at the ion's position. For the plasmon dispersion relation $\omega_s(q)$ in Al we have fitted the experimental data of Tsuei *et al.* [17] by means of the quadratic function $\omega_s(q)=\omega_s^0+\alpha q+\beta q^2$ with $\omega_s^0=0.4064$, $\alpha=-0.2938$, and $\beta=1.1430$.

The initial electron states can be written as

$$|\Phi_{\mathbf{k}}^{(i)}\rangle=e^{i\mathbf{k}_\rho\cdot\boldsymbol{\rho}}F_{k_z}(z), \tag{5}$$

with $\mathbf{k}_\rho(k_\rho,\varphi_k)$ and k_z the components of the initial electronic momentum parallel and perpendicular to the surface plane, respectively, and where the z-dependent part $F_{k_z}(z)$ has been obtained numerically, by means of the Numerov algorithm, as the eigenfunction of the Hamiltonian

$$H_i^{(J)}=-\tfrac{1}{2}\nabla^2+V_{e\text{-}s}^J, \tag{6a}$$

$$V_{e\text{-}s}^J=-\frac{1-e^{-\lambda(z+s)}}{4(z+s)}\Theta(z+s)-\frac{V_0}{(Ae^{B(z+s)}+1)}\Theta(-z-s), \tag{6b}$$

where the potential $V_{e\text{-}s}^J$, defined by Jennings, Jones, and Weinert [18], takes properly into account the electron-surface interaction with $A=4V_0/\lambda-1$, $B=2V_0/A$, Θ being the unit step function and $\lambda=1$ a.u. for Al. In Eqs. (6) we do not include the perturbation of the initial metal electron states due to the interaction with the incoming ion. As in Ref. [11] we expect this to be a reasonable approximation due to the weakening of the electron-ion interaction as a consequence of screening. In fact, in recent calculations of collective rates for the H^+/Mg system [19] we have obtained, by application of a rather crude approximation, that the ion perturbation has a non-negligible contribution to the rates only in regions (not too close to the surface) where the collective rates themselves are very small compared to the rates near to the surface. Furthermore, in Ref. [12] they have found that for the $He^+(1s)$/Al system the effect of the perturbation of the initial electron states (due to the presence of the ion) on the Auger neutralization rates start to be noticeable for ion-surface distances beyond $s\sim5$ where the corresponding Auger rates are more than three orders of magnitude smaller than those around $s\sim2$. Therefore, in order to avoid introducing unnecessary complications into the present calculations, we shall partially include this effect in our calculations by orthogonalizing the initial electron states with respect to the final bound electron state, which takes into account the ion-surface interaction as we indicate in what follows.

For the collective surface-plasmon channel the only relevant final bound electron state is the ground state of He, since, the energy released during an electron capture into any of its higher levels is not enough to excite a surface plasmon. For the ground state of He atom in front of the Al surface, we consider the Hamiltonian

$$H_f=-\tfrac{1}{2}\nabla^2+V_{e\text{-}s}^J+V_{e\text{-}i}+\Delta V, \tag{7}$$

$$V_{e\text{-}i}(r)=-\frac{1}{r}-\left(4+\frac{1}{r}\right)e^{-4r}-\sum_{j=1}^{4}c_j r^{j-1}e^{-2r}, \tag{8}$$

$$\Delta V(\rho,z)=\frac{\theta(z+s)}{\sqrt{\rho^2+(z+2s)^2}}, \tag{9}$$

with $r=\sqrt{\rho^2+z^2}$ ($c_1=-8.9595$, $c_2=29.4240$, $c_3=-20.8924$, $c_4=3.6381$). In Eq. (7) $V_{e\text{-}s}^J$ is the electron-surface interaction of Jennings, Jones, and Weinert [18], already given in Eq. (6), $V_{e\text{-}i}$ is the intra-atomic electron-core interaction described through the Bottcher (singlet) potential [20], which reproduces pretty well the observed energy levels of the isolated He atom and ΔV is the usual electron-ion (image) potential, which takes into account the change in the electron-surface interaction due to the presence of the positive ion.

The calculation of the eigenvalues and the corresponding eigenfunctions $|\Phi_n^{(f)}\rangle$ of H_f proceeds by diagonalization of a basis set of hydrogenic parabolic orbitals $u_{n_1,n_2,m}(\rho,\varphi,z)$ [21] [with the principal quantum number n^* related to the parabolic quantum numbers (n_1,n_2,m) by $n^*=n_1+n_2+m+1$]. The eigenfunctions are written as linear combinations of the basis orbitals:

$$|\Phi_n^{(f)}\rangle=\sum_{i=1}^{N}C_{ni}(s)|u_i\rangle, \tag{10}$$

where the dependence on the ion-image plane distance s is due to the interaction between the final atomic state and the various image charges. In Eq. (10), the size of the basis set (N) is increased until the eigenvalues are independent (within the desired accuracy) of the number of basis orbitals. To represent the ground state of He in front of the Al surface, we have checked that it is sufficient to include in expansion (10) $N=6$ hydrogenic parabolic orbitals (i.e., all the $m=0$ orbitals up to the $n^*=3$ shell). It is found that the energy shifts for the ground state follow an image charge behavior $1/4s$ even up to distances $s=2$ where it reaches a value of 3.5 eV [21].

With all the above, the transition rate of Eq. (2) becomes

$$\Gamma^{n}_{\mathrm{PSP}}(s,v_{\parallel})=\frac{1}{8\pi^3}\int_{q_{\min}}^{q_{\max}}dq\,\omega_s(q)\int_0^{\sqrt{2E_F}}dk_\rho k_\rho \times\int_0^{2\pi}d\varphi_k\,\theta\left(\varepsilon_f(s,q)-\frac{1}{2}\chi_\parallel^2\right) \times\frac{1}{k_z}\,\theta\left(\frac{1}{2}(k_F^2-k_\rho^2)+\frac{1}{2}\chi_\parallel^2-\varepsilon_f(s,q)\right) \times\int_0^{2\pi}d\varphi_q\,|\tilde{\mathcal{M}}^{n,\mathbf{q}}_{\mathbf{k},\mathbf{v}_\parallel}(k_z,k_\rho,\varphi_k,q,\varphi_q;v_\parallel,s)|^2, \tag{11}$$

with $\chi_\parallel^2=k_\rho^2-2k_\rho v_\parallel\cos(\varphi_k)+v_\parallel^2$ and $k_z=\sqrt{2\varepsilon_f(s,q)-\chi_\parallel^2}$, and where the matrix element $\tilde{\mathcal{M}}^{n,\mathbf{q}}_{\mathbf{k},\mathbf{v}_\parallel}$ is

$$\tilde{\mathcal{M}}^{n,\mathbf{q}}_{\mathbf{k},\mathbf{v}_\parallel}=\sum_{j=1}^{N}C_{nj}(s)\tilde{\mathbf{M}}_j^{(1)}(k_z,k_\rho,\varphi_k,q,\varphi_q,v_\parallel,s) -\sum_{m=1}^{\mathcal{P}}\left\{\left[\sum_{i=1}^{N}C_{mi}(s)\tilde{\mathbb{O}}_i(k_z,k_\rho,\varphi_k;v_\parallel,s)\right] \times\left[\sum_{j=1}^{N}\sum_{i=1}^{N}C_{mi}(s)C_{nj}(s)\mathbf{M}_{ij}^{(2)}(q)\right]\right\}. \tag{12}$$

The matrix elements $\tilde{\mathbb{M}}_j^{(1)}=\langle u_j|e^{-q|z+s|}e^{-i\mathbf{q}\cdot\boldsymbol{\rho}}e^{-i\mathbf{v}_\parallel\cdot\boldsymbol{\rho}}|\Phi_{\mathbf{k}}^{(i)}\rangle$, $\tilde{\mathbb{O}}_i=\langle u_i|e^{-i\mathbf{v}_\parallel\cdot\boldsymbol{\rho}}|\Phi_{\mathbf{k}}^{(i)}\rangle$ and $\mathbb{M}_{ij}^{(2)}=\langle u_i|e^{-q|z+s|}e^{-i\mathbf{q}\cdot\boldsymbol{\rho}}|u_j\rangle$ are calculated numerically by means of Gauss-Laguerre and Gauss-Legendre quadratures. In Eq. (12), $\mathcal{P}$ corresponds to the number of final atomic eigenfunctions included in the orthogonalization procedure. In the present calculation, the initial state $|\Phi_{\mathbf{k}}^{(i)}\rangle$ is orthogonalized to the perturbed ground state of He, i.e., to the final bound electron state $|\Phi_n^{(f)}\rangle$. It is important to note that the conservation of the energy and the constraints $0\leqslant k\leqslant k_F$ (k_F being the Fermi wave vector modulus) for the metal electron wave vector fix the limits $q_{\min}$ and $q_{\max}$ of integration over q appearing in Eq. (11) through the two unit step functions $\Theta(x)$ appearing in the integration over φ_k.

B. Neutralized fractions and angular distributions

If one neglects the population of excited states of He atoms, the occupations corresponding to the ground state of the ion (P_+) and to the ground state of the neutral atom (P_g) are given by the following set of coupled rate equations:

$$dP_+(t)/dt=-\Gamma_G(s,v_\parallel)P_+(t),$$
$$dP_g(t)/dt=+\Gamma_G(s,v_\parallel)P_+(t). \tag{13}$$

The transition rate $\Gamma_G(s,v_\parallel)$ represents the contributions to the neutralization into the ground state, i.e., the PSP rates $[\Gamma_{\mathrm{PSP}}(s,v_\parallel)]$ or the multielectron Auger rates $[\Gamma_{\mathrm{MEA}}(s)]$. The PSP rates are those obtained as indicated in the preceding section. For the MEA rates, we have used those from Refs. [12,13].

As these transition rates are calculated as functions of the ion-image plane distance s, in order to integrate the set of coupled rate equations, we use the transformation

$$dt=\frac{ds}{v_{i\perp}(s)}, \tag{14}$$

where $v_{i\perp}(s)$ is the perpendicular velocity of the ion. This velocity is computed by means of energy conservation for the ion motion:

$$v_{i\perp}(s)=\sqrt{\frac{2}{M_I}}\sqrt{E_{\perp 0}-U_T(s)}, \tag{15}$$

with M_I the ion mass, $E_{\perp 0}$ its total energy corresponding to the normal motion, and $U_T(s)$ the total scattering potential experienced by the ion, which can be written as the sum of a repulsive potential $U_R(s)$ due to the first atomic plane and an attractive potential $U_A(s)$ produced by the interaction of the ion with its own image charge:

$$U_T(s)=U_R(s)+U_A(s). \tag{16}$$

The repulsive term $U_R(s)$ is obtained as described in Gemmel's review [22] by averaging over the first atomic plane individual interatomic potentials. In the present work, the interatomic potential is represented by a ZBL screening function [23]. For the attractive image potential $U_A(s)$, we have used the form based on the Thomas-Fermi approximation proposed by Kato, Williams, and Aono [24]. The explicit form for all these potentials and their related parameters have been given in Ref. [11].

By means of the transformation of Eq. (14) the rate equation system of Eq. (13) becomes

$$dP_+(s)/ds=-\Gamma_G(s,v_\parallel)P_+(s)/v_{i\perp}(s),$$
$$dP_g(s)/ds=+\Gamma_G(s,v_\parallel)P_+(s)/v_{i\perp}(s). \tag{17}$$

These coupled equations are integrated (by means of a Runge-Kutta method) for the incoming and the outgoing paths with the initial conditions $P_+^{in}(s\to+\infty)=1$ and $P_g^{in}(s\to+\infty)=0$ and the normalization $P_+(s)+P_g(s)=1(\forall s)$.

In order to obtain the angular distribution of scattered neutral atoms in the ground state, we calculate for each integration interval ds of Eq. (17), the elementary fraction of ions that are neutralized in the ground state (i.e., dP_g). For very low perpendicular velocities like those considered here, there is no reionization mechanism in close encounter collisions. Moreover, for the collision investigated in the experimental work of Hecht, Winter, and Borisov [10], with respect to which we want to compare our results, the parallel velocity $v_\parallel=0.14$ a.u. is not large enough to allow a loss mechanism like that proposed by Winter [9]. Therefore, once the ground state is populated, the He atoms cannot experiment further transitions, remaining as neutral He($1s^2$) atoms. At the instant of neutralization, the attractive image potential vanishes and then, the neutral atoms in the ground state feel only the planar potential. The corresponding outgoing angle φ is given by the composition of the parallel velocity $v_\parallel$

(which is a constant here because corrugation effects are not considered) and the asymptotic perpendicular velocity of neutral atoms in the outgoing path $v_{g\perp}^{out}$,

$$\tan\varphi = \frac{v_{g\perp}^{out}}{v_{\parallel}}, \tag{18}$$

where $v_{g\perp}^{out}$ is obtained by means of energy conservation for neutrals in the repulsive potential:

$$v_{g\perp}^{out} = \sqrt{v_{i\perp}^2(s^*) + \frac{2}{M_g}U_R(s^*)}, \tag{19}$$

where M_g is the mass of neutral particles, $v_{i\perp}(s^*)$ is the perpendicular velocity acquired by the ion at the distance corresponding to its neutralization (s^*), and $U_R(s^*)$ is the value of the planar potential at this distance.

Angular distributions are obtained by arranging the elementary neutral fractions dP_g according to their outgoing angle. The convergence of this approach might be checked by decreasing the integration step ds (tipically here, $ds \approx 5 \times 10^{-3}$ a.u. to obtain accurate results). Afterwards, the theoretical angular distribution is convoluted by means of a Gaussian shape of width $\delta\varphi = 0.08°$ in order to account for the experimental angular resolution [10]. Finally, the angular distributions presented below are normalized in such a way that their area correspond to the fraction of scattered atoms in the ground state [i.e., $P_g^{out}(s \to +\infty)$]. The experimental angular distribution [10] was normalized in the same way.

Recently [25], we have developped a more general (and also more cumbersome) approach to compute atomic and ionic fractions and also angular distributions of scattered particles. This method, which is of classical trajectory Monte-Carlo (CTMC) type, is based on the integration of Hamilton-Jacobi equations for the particles motion and takes into account the charge exchange mechanisms with the corresponding changes in the potentials felt by the particles when an electronic transition occurs. In the particular case considered here—one kind of electronic transition towards an atomic state, which cannot experiment further charge exchange mechanisms—the simpler and faster rate equation method presented above and the more general CTMC one yields the same results both for charge fractions and angular distributions.

III. RESULTS AND DISCUSSION

A. Atomic description effects for collective transition rates

In our previous work for the He^+/Al system [11] we reported PSP rates within the FIA and applied them to obtain angular distributions for the final neutralized helium ions. The main concern in that work was to study the contribution of the surface-plasmon mode of neutralization to the angular distribution of the final neutral He atoms so that only few details were given about the calculated PSP rates. In particular, the effects of the representation of the final atomic state were not studied there. Therefore, in this section we analyze the dependence of our PSP rates on different approximations introduced to describe the atomic wave function representing the final bound state of the neutralized ion for the He/Al system. In Fig. 1(a) we show three PSP neutralization rate curves $\Gamma_{PSP}^{(i)}$ $(i=1,2,3)$, as functions of the ion-image plane distance s, for three different approximations of the atomic wave function in which the terms with $n^*=1$, 2, 3, respectively, have been kept in the expansion given by Eq. (10). At small ion-surface distances the three curves go close to each other, showing a similar behavior with ion-surface distance. Around $s \sim 3$ they start to develop an approximate exponential decay, but near $s=5$ the rates $\Gamma_{PSP}^{(2)}$ and $\Gamma_{PSP}^{(3)}$ get an important change of slope, which diminish their decay, remaining close to each other and much higher than $\Gamma_{PSP}^{(1)}$, which mantains its exponential decay up to infinity. Around $s \sim 7$ the rates $\Gamma_{PSP}^{(2)}$ and $\Gamma_{PSP}^{(3)}$ start to develop again an approximate exponential behavior, although with a smaller slope than that showed by $\Gamma_{PSP}^{(1)}$, but near $s \sim 9$ $\Gamma_{PSP}^{(3)}$ changes its slope once again while the curve $\Gamma_{PSP}^{(2)}$ keeps its (second) exponential descense in such a way that at large distances $\Gamma_{PSP}^{(3)} \gg \Gamma_{PSP}^{(2)} \gg \Gamma_{PSP}^{(1)}$.

As a consequence of this behavior at $s \sim 9$ the curve $\Gamma_{PSP}^{(1)}$ is two orders of magnitude smaller than the other two curves while at $s \sim 15$ the rate $\Gamma_{PSP}^{(2)}$ is 20 times smaller than $\Gamma_{PSP}^{(3)}$. The slow decay of our pure surface plasmon transition rates at intermediate and large ion-surface distances is directly related to the higher-order contributions to the expansion of the final atomic state given by Eq. (10). Indeed, the variation of the slope of $\Gamma_{PSP}^{(2)}$ and $\Gamma_{PSP}^{(3)}$ around $s=5$ can be unambiguously related to the contributions from the $n^*=2$ shell, which at this distance start to be more important than the contribution coming from the $n^*=1$ shell. In fact, the expansion of Eq. (10) for the eigenfunctions is strongly dominated at very short distances by the first term but it decays too fast with s as compared to the second term, which starts to become noticeable around $s \sim 4$ and taking over around $s=5$. A second slope variation occurs to $\Gamma_{PSP}^{(3)}$ starting at $s \sim 9$ and becoming very clear at $s \sim 10$, which is related to the fast decay of the $n^*=2$ as compared to the $n^*=3$ terms in the expansion that contribute more than the other terms around this distance.

From the precedent discussion, one can visualize a simple picture of the electron capture where the largest hydrogenlike orbitals included in the expansion of Eq. (10) reach first the surface inducing the electron capture at large ion-surface distances. In particular, the average radius of the $n^*=2$ and the $n^*=3$ hydrogenic shells are approximately 4 a.u. and 9 a.u., respectively, which correspond to the distances at which the $n^*=2$ and the $n^*=3$ shells start to contribute notoriously to the total collective rate $\Gamma_{PSP}^{(3)}$. In this sense, the average radius of every state in the expansion might allow one to estimate the distance at which each term in the expansion is going to become more important than the precedent term. Furthermore, the average radius of the $n^*=1$ shell is approximately 1 a.u. being very close to the value of the distance at which the PSP rate gets its highest value (before vanishing due to the energy conservation restriction and the shift of the atomic energy level). Therefore, within this picture the neutralization probability at large distances is very

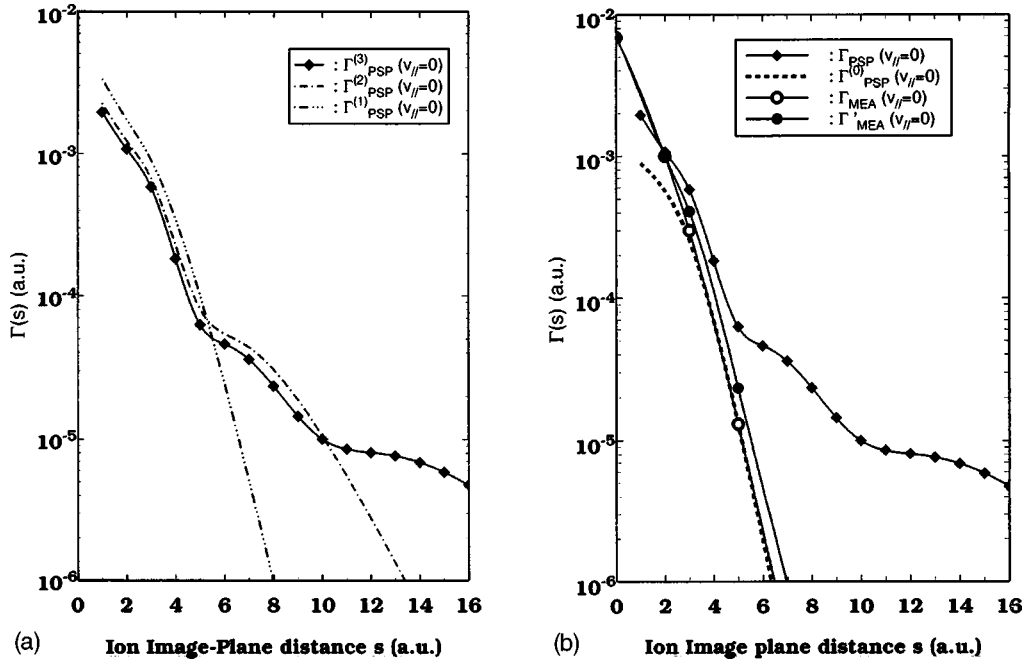

FIG. 1. PSP and MEA transition rates as a function of the ion-image plane distance. (a) ♦, PSP transition rate calculated by including in Eq. (10) all the $m=0$ orbitals up to $n^*=3$ $[\Gamma^{(3)}_{\rm PSP}(v_\parallel=0)]$; dashed-dotted line, the expansion of Eq. (10) is restricted to the $n^*=1$ and $n^*=2$ orbitals $[\Gamma^{(2)}_{\rm PSP}(v_\parallel=0)]$, dashed-triple dotted line: the expansion is restricted to the $n^*=1$ orbital only $[\Gamma^{(1)}_{\rm PSP}(v_\parallel=0)]$. (b) ♦, $\Gamma^{(3)}_{\rm PSP}(v_\parallel=0)$; dashed line, PSP transition rate computed by using a description of the final atomic state similar to that used in Refs. [12,13] for the MEA rates $[\Gamma^{(0)}_{\rm PSP}(v_\parallel=0)$, see text]; ○ and ●, MEA transition rates calculated in Refs. [12,13] (○, ●, with and without inclusion of the ion effect on the initial electronic wave function, respectively).

small compared to the same probability at short distances because the weight of the largest orbitals in the expansion of the perturbed wave function is much smaller than the weight of the smallest orbitals.

The small differences between our three curves $\Gamma^{(i)}_{\rm PSP}$ $(i=1,2,3)$ at short distances are related to the fact that the energy for every curve is obtained consistently with the wave function, so that the better is the description of the wave function the better is the energy. Together these two effects are responsible for the small increment of the collective rates at short distances where the perturbation of both energy and wave function for the atomic state is largest. Note, however, that for $s\lesssim 4$ the differences between $\Gamma^{(2)}_{\rm PSP}$ and $\Gamma^{(3)}_{\rm PSP}$ are notoriously smaller than the differences between $\Gamma^{(1)}_{\rm PSP}$ and $\Gamma^{(2)}_{\rm PSP}$. Therefore, the convergence of the wave function expansion yields a convergence of the collective rates to a final curve which differs from $\Gamma^{(3)}_{\rm PSP}$ by less than 1% for $s\leqslant 20$. Therefore, in the rest of this paper we shall take $\Gamma^{(3)}_{\rm PSP}\equiv\Gamma_{\rm PSP}$.

In order to find out the source of the discrepancy between our FIA surface plasmon rates and the MEA rates, we show in Fig. 1(b) another approximated PSP rate, denoted as $\Gamma^{(0)}_{\rm PSP}$, which considers a $1s$-hydrogenlike wave function to describe the final atomic state (where the parameter $\alpha=1.34$ yields the best energy for the ground state at infinity). In the evaluation of $\Gamma^{(0)}_{\rm PSP}$ the $1s$-hydrogenlike wave function remains frozen for all ion-surface separations, although the energy is shifted according to the classical $1/4s$ behavior. These approximations are very similar to those involved in the evaluation of the MEA rates [12,13], which we include in Fig. 1(b). The rate $\Gamma_{\rm MEA}$ ($\Gamma'_{\rm MEA}$) corresponds to calculations performed with unperturbed (perturbed) initial electron states where the perturbation is caused by the field of the nearby He^+ ion. For comparison purposes we also include in Fig. 1(b) our best PSP rate $\Gamma_{\rm PSP}$. As mentioned in the introduction a very important feature of the multielectron neutralization rates is that they include simultaneously both the collective and the single particle response of the metal surface. We note first that the curve $\Gamma^{(0)}_{\rm PSP}$, which is very different from $\Gamma_{\rm PSP}$ in the whole range of distances, is very close to the rate $\Gamma_{\rm MEA}$, especially for $s\gtrsim 3$. The very small differences between $\Gamma^{(0)}_{\rm PSP}$ and $\Gamma_{\rm MEA}$ at large distances are due to the different choices of the variational parameters included for the atomic wave functions. Second, we note that in Ref. [5] they have concluded that despite the fact that the calculation of $\Gamma_{\rm MEA}$ includes all possible neutralization channels, the determining neutralization channel at distances greater than 3 a.u. from the surface is the monopole surface plasmon channel. Therefore, from these facts we are led to the conclusion that $\Gamma^{(0)}_{\rm PSP}$ and $\Gamma_{\rm MEA}$ contain the same surface-plasmon contribution. Since the only difference between $\Gamma^{(0)}_{\rm PSP}$ and $\Gamma_{\rm PSP}$ is the more precise description of the final atomic wave function in the evaluation of the latter we believe that $\Gamma_{\rm PSP}$ contains the same surface-plasmon contribution as $\Gamma_{\rm MEA}$. In other words, if our atomic wave function for the ground state of helium were included in the evaluation of $\Gamma_{\rm MEA}$, the resulting curve should be very close to $\Gamma_{\rm PSP}$ for the range $s\geqslant 3$. These conclusions also indicate that the model Hamiltonian of Eq. (4)

is quite appropriate to describe the electron-surface-plasmon coupling for ion-surface distances in the range $s \gtrsim 3$. Finally, by comparison of Γ'_{MEA} with both $\Gamma^{(0)}_{\mathrm{PSP}}$ and Γ_{PSP} in Fig. 1(b) we can conclude that the perturbation of the initial metal electron states by the incoming ion produces an effect that is small as compared to the effect of describing appropriately the final atomic state for the helium atom.

We note that although our curve $\Gamma^{(1)}_{\mathrm{PSP}}$ [given in Fig. 1(a) but not shown in Fig. 1(b)] goes above both $\Gamma^{(0)}_{\mathrm{PSP}}$ and Γ_{MEA}, it also shows a similar (nearly parallel) decay behavior in the range $s \gtrsim 3$. The explanation is that to obtain $\Gamma^{(1)}_{\mathrm{PSP}}$ only the first term in the expansion of Eq. (10) was kept, which at large distances is equivalent to describe the perturbed ground state of the helium atom by a $1s$-like type of wave function. At small distances the first term in the expansion of Eq. (10) is affected by the surface, an effect not included in the evaluations of both $\Gamma^{(0)}_{\mathrm{PSP}}$ and Γ_{MEA} where the corresponding exponential wave functions were kept frozen. However, the main difference between $\Gamma^{(1)}_{\mathrm{PSP}}$ and $\Gamma^{(0)}_{\mathrm{PSP}}$ comes from the fact that in the calculation of $\Gamma^{(1)}_{\mathrm{PSP}}$ the energy of the final state has been computed for all distances consistently with the wave function leading to a poor description of the energies because in that case the expansion of Eq. (10) contains only one term, while for $\Gamma^{(0)}_{\mathrm{PSP}}$ and Γ_{MEA} the energies have been (unconsistently) fixed to their correct values.

B. Collective versus single particle neutralization

In this section we present a simple argument to illustrate why, for those ion-metal systems where potential emission of a surface plasmon is energetically allowed, it is reasonable to expect the collective transition rate to be much larger than the two-electron Auger rate at intermediate and large ion-surface distances. We start by noticing that, in general, for simple (electron gas) metals, such as Al, the surface-plasmon energy is very close to (and sometimes slightly larger than) the Fermi energy. Therefore, to have enough energy to produce a real surface plasmon during the neutralizing transition, the metal electron should be captured into an atomic level located below the bottom of the conduction band [26]. Energy conservation requires the absorption of the released energy by another participant in the process, which can be a second electron (in the two-electron Auger mode) or a surface-plasmon (collective multielectron surface mode). Since in the Auger transition only one electron absorbs all the energy liberated during the capture, it means that the rest of the electrons of the metal should not become aware of it. By the contrary in the collective case the energy liberated during the capture has to be shared simultaneously by many electrons to give rise to surface-density fluctuations whose quanta are the surface plasmons. To discriminate between these two possible neutralization modes, it is relevant to find out how the interaction between the captured electron with a particular electron of the surface compares with the simultaneous interaction of the captured electron with many of the electrons at the surface.

Consider a He^+ ion fixed in front of an Al surface. It is clear that right after its capture into the ground state of helium $He^0(1s^2)$ the electron will be localized around the He^+ ion core within a distance of the order of the average radius of the ground level, which in our case is approximately 1 a.u. Then if the ion is fixed at a large distance from the metal surface ($s \gg 1$) the bound electron, denoted as e_b will also be far from the surface at a distance, which for practical purposes can be taken to be $\sim s$ along the z axis perpendicular to the surface. Consider next a sheet of electrons at the metal surface ($z=0$ plane) and draw a circle (C_ρ) of radius ρ centered on one of the sheet electrons, denoted as e^*, which is in front of e_b along the z direction (so that e^* is the surface electron closest to e_b). The interaction between e_b and e^* is $V(s)=1/s$, while the interaction between e_b and any other sheet electron, located on or inside C_ρ, is

$$U \geqslant \frac{1}{\sqrt{\rho^2+s^2}}, \tag{20}$$

so that one can write

$$\frac{V}{\sqrt{1+\left(\frac{\rho}{s}\right)^2}} \leqslant U \leqslant V. \tag{21}$$

The main idea here is to estimate the number $N(\rho)$ of electrons on or inside C_ρ whose interaction U with the captured electron e_b is not negligible as compared to the interaction V between e_b and e^*. If $N(\rho) \gg 1$ then clearly the captured electron will be more willing to give up its energy surplus through a collective channel instead of doing it through a single particle channel. Such number can be simply estimated as $N(\rho) \cong A/a - 1 = (\rho/r_s)^2 - 1$, where $A=\pi\rho^2$ is the area of C_ρ and $a=\pi r_s^2$ (for $\rho \geqslant r_s$) is the effective area on the $z=0$ plane for each electron on the sheet, with $r_s = (4/3\pi n_e)^{-1/3}$ where n_e is the electronic density of the solid. In the limit $s \to \infty$, one has that $U \to V$, for any value of ρ, so that for very large ion-surface distances the captured electron will interact equally with all the electrons of the metal and not with only one of them. For finite values of s we have to consider specific values of ρ for which U is not negligible as compared to V. For instance, when $\rho = 2s$, one has that $U \gtrsim 0.45V$, so that one cannot neglect these interactions. In this case for the set of distances $s/r_s = (2,5,10)$ one gets the numbers $N=(15,99,399)$. Thus, at these ion-surface distances the captured electron e_b interacts simultaneously with an appreciable number of surface electrons [27]. For the larger circle of radius $\rho = 10s$, one has $U \gtrsim 0.1V$, while $N = (400,2500,10\,000)$ for the ion-surface distances $s/r_s = (2,5,10)$. Clearly at intermediate and large ion-surface distances, the captured electron e_b interacts simultaneously with many surface electrons instead of interacting with just one of them. Therefore, whenever the energy released by the electron e_b during its capture into the atomic level is equal or larger than the surface-plasmon energy, the surface will be more willing to accept the surplus energy through a collective response (surface plasmons) than through a single-particle response.

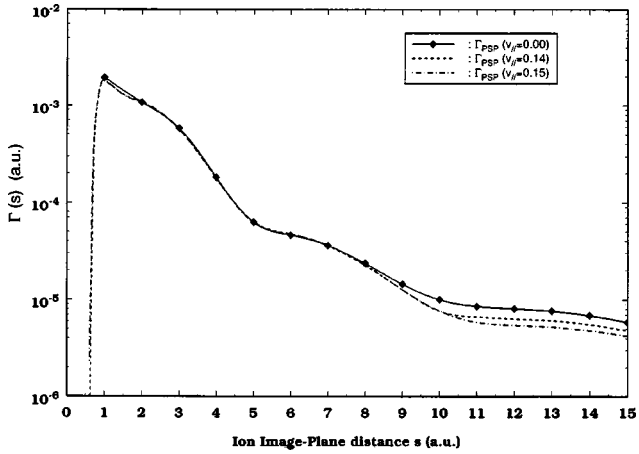

FIG. 2. PSP transition rates as a function of the ion-image plane distance. ◆, $v_{\parallel}=0$; dashed line, $v_{\parallel}=0.14$; dashed-dotted line, $v_{\parallel}=0.15$.

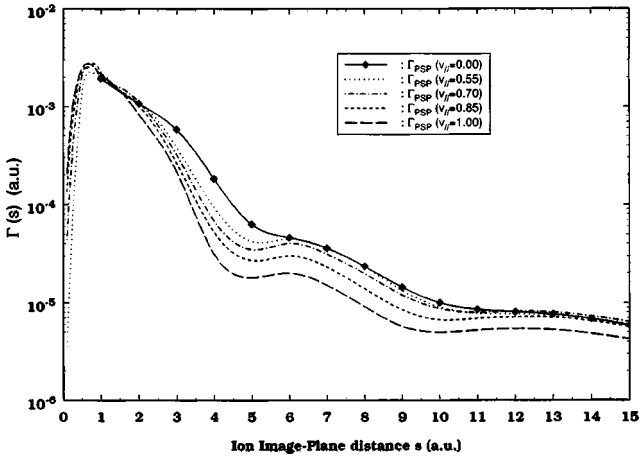

FIG. 4. PSP transition rates as a function of the ion-image plane distance. ◆, $v_{\parallel}=0$; dotted line, $v_{\parallel}=0.55$; dashed-dotted line, $v_{\parallel}=0.7$; dashed line, $v_{\parallel}=0.85$; long-dashed line, $v_{\parallel}=1$.

At short distances the plasmon emission is still possible but the probability for the two-electron Auger process gets high enough to compete with the collective mode. In fact, when $\rho/r_s \leqslant 1$, the number of surface electrons around e^* vanishes. In that case the captured electron e_b clearly identifies the electron e^* from all the other electrons, so that the single-particle mode can compete with the collective mode, which is present only up to a finite distance ($s \sim 0.5 r_s$ for the He^+/Al system) where conservation of energy makes the collective rate to vanish as already reported in Ref. [11].

C. Velocity effects for surface-plasmon transition rates

In Fig. 2–4 we show our PSP neutralization rates Γ_{PSP} for the $He^+(1s)-Al$ system as functions of the ion-image plane distance s for three different ranges of velocities. In Fig. 2 we compare our FIA collective rate [11] with those for parallel velocities $v_{\parallel}=0.14$ and 0.15, which are relevant to the experimental work of Ref. [10]. In Fig. 3 we extend the range of ion velocities up to $v_{\parallel}=0.40$, which is slightly below the threshold velocity ($v_{thr} \sim 0.42$) for kinetic surface-plasmon emission in Al (which occurs without electron capture), so that the velocity and the trajectory of the incoming ion, which are of crucial interest in the study of angular distributions for neutralized ions after grazing collisions with metallic surfaces, cannot be perturbed by this type of process. Finally, in Fig. 4, besides the FIA curve, we show our collective transition rates for the larger parallel velocity range $v=[0.55-1.0]$ where it is possible for the ion to loose energy by kinetic surface-plasmon emission although, for this range of velocities, the kinetic energy of the ion is more than a hundred times larger than the energy of the surface plasmon, so that this type of energy loss should perturb very weakly the ion's velocity. Before discussing the effects of the velocity on the collective transition rates and also on the corresponding angular distributions (following section) it is of relevance to note that the experimental angular distribution for the $He^+(1s)-Al$ system under a grazing incidence angle of 0.5° for 2 keV He^+ ions [10] covers the range of scattering angles [1.5°–3.5°] with the maximum of the angular distribution located around 2.45°. From the simple correlation between the scattering angle and the neutralization distance we can infer that (for the scattering potentials we are considering in this work, which are the same as those of Ref. [11]) most of the collective neutralizations occur within the range of distances $s=[0.5-8]$ with the maximum neutralization around $s \sim 2$.

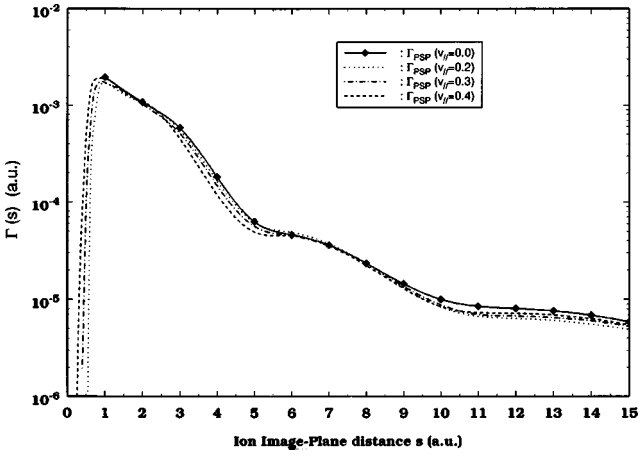

FIG. 3. PSP transition rates as a function of the ion-image plane distance. ◆, $v_{\parallel}=0$; dotted line, $v_{\parallel}=0.2$; dashed-dotted line, $v_{\parallel}=0.3$; dashed line, $v_{\parallel}=0.4$.

For $v_{\parallel} \leqslant 0.15$ Fig. 2 shows that within the range of distances $1 \lesssim s \lesssim 8$ the two velocity dependent PSP rates go on top of the curve obtained within the FIA, while for $s>8$, where all the rates are two orders of magnitude smaller than their maximum value near $s \sim 1$, they show a difference ($\lesssim 35\%$), which is clearly small as compared to their general decay behavior. The approximate independence of our calculated PSP rates with respect to the ion velocity in the range of distances $s \gtrsim 1$ where the FIA process is energetically allowed can be qualitatively understood from a simple analysis of the finite velocity matrix elements $\tilde{\mathbf{M}}_j^{(1)}$ of Eq. (12), which differ from the FIA case by the extra factor $\exp\{-i\mathbf{v}_{\parallel}\cdot\boldsymbol{\rho}\}$.

Symmetry considerations related to the fact that the ion velocity $v_\parallel$ has an arbitrary direction transforms this factor in $\cos(\mathbf{v}_\parallel \cdot \boldsymbol{\rho})$ which, for $\mathbf{v}_\parallel \cdot \boldsymbol{\rho} < 1$, a condition that is satisfied here, can be written approximately as $1 - \frac{1}{2} v_\parallel^2 \rho^2$. The first term yields the FIA results, while the second term contains the velocity effects. Take $v_\parallel \sim 0.15$, and consider first the case of small ion surface distances s for which the $n^* = 1$ orbital makes the most important contribution to Eq. (10). Therefore, since for the ground state the average value of r is $\langle r \rangle \sim 1$, the velocity effects are expected to be negligible at short ion-surface distances. On the other hand, for large ion-surface distances ($s \gtrsim 8$) the higher orbitals contributions in Eq. (10) (for which the average value of r is larger than 1) become more important, producing a noticeable effect on the velocity-dependent collective rates, as we see in Fig. 2. However, since for $s \gtrsim 8$ the PSP rates are at least two orders of magnitude smaller than near the surface, these velocity effects are of negligible consequences for the evaluations of neutral fractions although they produce clear effects on the collective angular distributions, as we shall see later.

For short distances $s < 1$ the FIA rate vanishes [11], while the collective rates Γ_{PSP} for $v_\parallel \neq 0$ remain finite, although they decay very fast toward smaller distances, being at $s = 0.5$ more than four orders of magnitude smaller than at $s = 1$. We shall see on the following section that the effect of the finiteness of the collective rates for $s < 1$ produces larger and more relevant effects on the corresponding angular distributions of the final neutrals than those coming from the range $s \gtrsim 8$ discussed in the preceding paragraph. The vanishing of Γ_{PSP} below a threshold distance $s_0 = 1$ [11] for the fixed ion case ($v_\parallel = 0$) is a direct consequence of the shifts of the bound-energy levels of He induced by the nearby metal surface, plus the constraint $k \leqslant k_F$, which makes it impossible the conservation of the energy for the collective process when $s < s_0$. The inclusion of the parallel velocity of the ion introduces enough initial energy to compensate the shifts of the bound atomic level, allowing the conservation of the energy and the existence of the collective channel at short ion-image plane distances.

In Fig. 3 the curves for $v_\parallel = 0.2$, 0.3, and 0.4 also go close to the FIA rate except in the intermediate range of distances ($2.5 \leqslant s \leqslant 5.5$) where they go slightly below the FIA rates with a relative difference, which is at most of 35% around $s = 4$ for $v_\parallel = 0.4$, being even smaller for $v_\parallel = 0.3$. These differences are still small as compared to the near exponential decay behavior of all these curves with s. As an example at $s = 4$ the rate Γ_{PSP} ($v_\parallel = 0$) is one order of magnitude smaller than Γ_{PSP} ($v_\parallel = 0$) at $s = 1$ so that differences smaller than 35% between the curves near $s = 4$ are negligible. Furthermore, a few checkings show us that these differences in the PSP rates yield differences in the corresponding neutralized He fractions, which are below 2% up to velocities $v_\parallel = 0.55$. This situation can be explained by the fact that neutralization occurs mostly near $s \simeq 2$ [11] where all the curves go very close. A peculiar feature of these velocity-dependent curves is that in those regions of s where one of the terms dominates the expansion of Eq. (10), the velocity effects are negligible, while in those region where the same term decays the velocity effects grow up to the point where the next term in the expansion takes over. A possible explanation, in terms of the simple picture of a set of orbits (related to the ion) interacting with the surface, might be that when one of the orbits ''touches'' the surface there are always electrons with the right momentum to match the ion velocity so that for many electrons the ion seems to be at rest; when the orbit gets outside of the surface this matching is not possible so that the velocity effect comes into play until the next orbit touches the surface where the velocity effect vanishes again, and so on.

Finally, in Fig. 4, besides the FIA curve we show our collective transition rates for the extended range of ion velocities $0.55 \leqslant v_\parallel \leqslant 1.00$. We distinguish two situations.

(1) For velocities $v_\parallel \lesssim 0.7$ the behavior of the finite velocity curves maintains a similar trend as those considered in Fig. 3. Now, however, the curves begin to separate a little closer to $s = 2$ with the largest difference located again near $s = 4$ where the rate for $v_\parallel = 0.7$ is decreased by an approximate factor of 1/3 with respect of the FIA rate, yielding a maximum relative difference of 65%. For $s \gtrsim 6$ these curves remain very close to the FIA curve with a negligible difference.

(2) For velocities larger than 0.7 the situation gets more complicated because once the curves get separated at or below $s = 2$ they do not merge at $s = 6$ as the curves for smaller velocities (approximately) do. In particular, the curve for $v_\parallel = 1.0$ is a factor of 1/4 smaller than the FIA rate at $s = 3$ and a factor 1/6 at $s = 4$. Therefore, we believe that in these cases there is a real effect of the ion velocity on the surface-plasmon transition rates, which is not negligible for the whole range of ion-surface distances where the collective neutralization is important.

D. Velocity effects for angular distributions

In order to illustrate how much the angular distributions, induced by the surface-plasmon mode of neutralization, are affected by the parallel velocity of the incoming ions we have considered the velocity-dependent transition rates obtained in the preceding section to solve the set of coupled equations (17) together with the appropriate initial conditions to obtain velocity-dependent angular distributions for the $He^+(1s)/Al(111)$ system. We assume here the conditions considered in the grazing incidence experiments of Ref. [10], where the ion beam has an energy of 2 keV with an angle of incidence of 0.5°, which amounts to a parallel velocity $v_\parallel = 0.14$, to obtain the angular distribution [AD(0.14)] shown in Fig. 5 (full line), which yields a neutral fraction of 74.2%. For comparison purposes, the analogous angular distribution for the same system and geometry but within the fixed ion approximation [AD(FIA)], reported in Ref. [11], which yields a neutralized fraction of 72.8% is also included in Fig. 5 (dotted line) together with the experimental curve of Ref. [10] (filled squares). Finally, we display in Fig. 5 the angular distribution obtained by consideration of the MEA rate of Ref. [12] (dashed line). We should remind at this point that all the theoretical as well as the experimental angular distri-

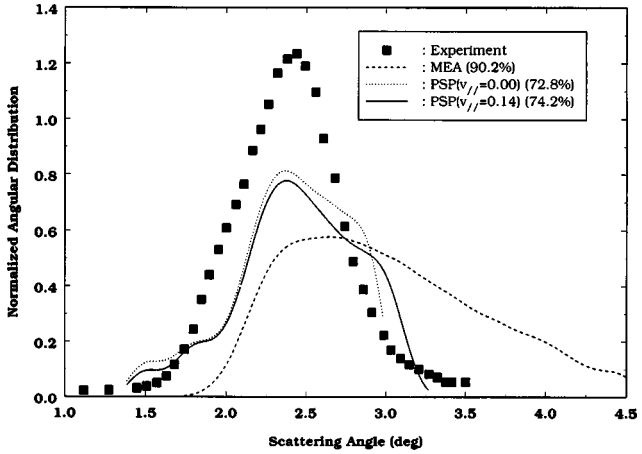

FIG. 5. Normalized angular distribution of scattered neutral He atoms as a function of the scattering angle $(\phi_{in}+\varphi)$ for 2 keV $He^+(1s)$ ions, impinging on an Al(111) surface with $\phi_{in}=0.5°$. ■, experimental result of Ref. [10] normalized to 100%; dashed line, theoretical result obtained by using the MEA rates of Refs. [12, 13]; dotted line, theoretical result obtained by using the PSP rates computed in this work for $v_{\parallel}=0$; full line, theoretical result obtained by using the PSP rates computed in this work for $v_{\parallel}=0.14$.

butions presented here have been normalized in such a way that their area corresponds to the fraction of scattered atoms in the ground state.

A first conclusion one can obtain is that although the velocity effects on the collective rate Γ_{PSP} for $v_{\parallel}=0.14$ were found to be small with respect to the FIA, the corresponding effects on the angular distributions appear to be larger and more relevant. This is not the case for the related neutralized fractions, which show a relative difference of 1.9%. We can also see that for small angles (where the left tail of both calculated angular distributions go above the experimental one) the velocity-dependent angular distribution goes below the FIA curve, something that is consistent with the fact that the velocity-dependent collective rate goes below the FIA rates for distances above $s=8$. Clearly, this is an small effect. For larger angles the AD(FIA) still goes above the AD(0.14) but start to decay faster than it after they reach their maximum. The AD(FIA) crosses from above the AD(0.14) at $\varphi_s=2.9°$, remaining below it before vanishing drastically at $\varphi_s=2.98°$ as a consequence of the vanishing of the FIA transition rate below $s=1$. As already mentioned before the energy related to the parallel ion velocity allows the existence of the surface-plasmon mode below the FIA threshold so that the velocity-dependent angular distribution does not vanish abruptly as in the FIA case, but gets wider than the FIA distribution, remaining finite and decreasing smoothly to small values up to the angle $\varphi_s=3.26°$ beyond which it vanishes. The increment on the width of the velocity-dependent angular distribution is a result of the fact that since now some neutralizations can occur closer to the surface therefore, the dynamical effects (of the attractive potential before the neutralization plus the repulsive potential after the neutralization) yield an increment of the outgoing angle, producing an increment in the population of neutrals at larger angles.

The width difference between the MEA and the PSP angular distributions are related to the large values of Γ_{MEA}—as opposed to the vanishing values of Γ_{PSP}—very close to the surface, where the image potential has its strongest effect. In fact, for an incident ion the large increment of $\mathbf{v}_{\perp}$ in the region $s\leqslant 1$ produces a large ''final angle of incidence'' at the neutralization position, which yields to a large outgoing angle for the neutralized particle. Since the rate Γ_{MEA} is largest in this region most of the neutralized ions will be sent to large angles. By the contrary, for distances $s\leqslant 1$, the PSP mode has a vanishing rate, due to energy constraints plus the upward shift of the bound atomic level, so that the PSP mode neutralizes particles not too close to the surface where the image potential is not strong enough to send the particles to large angles. The fact that the MEA angular distribution clearly overcomes the experimental curve at large angles might be taken as an indication of a possible overestimation of the MEA rate near the surface [11]. On the other hand, the differences both in shape and in neutral fraction between the PSP and the experimental angular distributions are expected to decrease after consideration of other contributions—besides the one coming from the PSP mode—to evaluate the theoretical angular distribution. Indeed, we expect that a more precise evaluation of the Auger rate, especially near the surface, should give a contribution which, when added to the PSP one, should yield a theoretical angular distribution closer to the experimental one. Furthermore, two other possible neutralization processes, which should be analyzed since their contribution might not be negligible, are those involving either the excitation of volume plasmons or the excitation of multipole surface plasmons as already mentioned in Ref. [28].

Our results, together with the precedent discussion, clearly illustrate the sensitivity of the angular distributions to the transition rates in the whole range of ion-surface distances. A similar conclusion for the ion-surface and atom-surface interaction potentials has been recently obtained [28]. Therefore, the information contained in the experimental angular distributions constitutes a reliable tool to test transition rates together with ion-surface interaction potentials. Finally, we mention that the main conclusion of Ref. [11], with respect to the importance of the surface-plasmon mode of ion neutralization during ion-metal surface electron exchange collisions, which were obtained within the FIA, is not changed by the inclusion of parallel ion velocities like those considered in the experiments of Ref. [10].

IV. CONCLUSIONS

In this work we have reported theoretical surface-plasmon transition rates for the neutralization of He^+ ions at Al surfaces. We have shown that for ion velocities $v_{\parallel}\lesssim 0.15$, typical of low-energy grazing incidence neutralizing collisions for He^+/Al like those of Ref. [10], these collective rates are practically independent of velocity validating in this way all the conclusions of Ref. [11], which were obtained within the FIA. In particular, the PSP collective rates lead to theoretical angular distributions, which are consistent with the experimental curves although other processes are needed to explain the full height of the experimental angular distributions. For velocities up to $v_{\parallel}\lesssim 0.7$, the velocity dependence shown by

the collective rates for an intermediate range of distances are small as compared to their near exponential decay behavior with ion-surface distance, so it should not produce measurable effects in the structure of electron emission spectra in qualitative agreement with recent experimental reports [7]. For $v_{\parallel} > 0.7$, the velocity effects seems to be important in the whole range of ion-surface distances where the surface-plasmon mode is of relevance for ion neutralization.

We have also shown in this work that although both the collective neutralization rate and the corresponding neutralized fraction depend very weakly on the parallel velocity in the energy range relevant for usual grazing incidence experiments, the effects on angular distributions of neutralized particles are noticeable. In this respect we would like to emphasize here that experimental angular distributions of scattered species after grazing interaction of an ionic (or atomic) beam with a surface [9,10] constitute a very precise tool to test both the theoretical transition rates for the relevant charge exchange processes as well as the related scattering potentials [28] for the ion-surface interactions.

On the other hand, we have been able to understand the discrepancy between the surface-plasmon neutralization rates of Ref. [11] and the multielectron Auger rates of Refs. [5], [12], [13]. It is related to the simpler representation of the final atomic wave function considered in Refs. [5], [12], [13], which leads to a strong underestimation of the multielectron Auger rates at intermediate and large ion surface distances. For the same range of distances a qualitative argument has been given to illustrate the fact that the collective mode of neutralization should be expected to be much more probable than the single particle Auger mode when the energy released during the electron capture is equal or larger than the surface-plasmon energy.

Finally, we mention a semiclassical interpretation for the potential emission of the surface plasmon during the ion-surface interaction. As indicated in the introduction the emission of a surface plasmon by a charged particle can occur if the velocity of the particle is larger than a threshold velocity $v_{thr} = \omega_{sp}/k_F$, which for Al yields $v_{thr} = 0.42$ a.u. For an electron this velocity corresponds to a kinetic energy of 2.4 eV, which is much smaller than the energy released by the electron exchange between the surface and the ion, and also much smaller than the energy necessary to produce a plasmon. The constraint imposed by the conservation of energy is much stronger than the threshold velocity condition so that any time that the plasmon emission is energetically allowed during ion neutralization, the velocity condition is automatically satisfied. Therefore, in a semiclassical picture of the emission, one of the surface electrons in the field of the ion increases its velocity until it trespasses the threshold velocity for plasmon emission, emits the surface plasmon, and gets bound to the ion.

ACKNOWLEDGMENTS

The collaboration between the Atomic Collisions Group at CELIA (Bordeaux, France) and FAG (Universidad de Concepción, Chile) was partially supported by the program ECOS/CONICYT, Grant No. C99E01, and also by the Project No. FONDECYT-1000311 (CHILE). The authors also wish to thank the Center de Resources Informatique (CRI) de l'Université de Bordeaux-I where the calculations were performed.

[1] R. W. Gurney, Phys. Rev. **47**, 479 (1935); J. W. Gadzuk, Surf. Sci. **6**, 133 (1967); **6**, 159 (1967).
[2] S. S. Shekhter, Sov. Phys. JETP **7**, 750 (1937); H. D. Hagstrum, Phys. Rev. **96**, 336 (1954); **122**, 83 (1961).
[3] A. A. Almulhem and M. D. Girardeau, Surf. Sci. **210**, 138 (1989).
[4] F. A. Gutierrez, Surf. Sci. **370**, 77 (1997); F. A. Gutierrez and J. Díaz-Valdéz, in *Surfaces, Vacuum, and Their Applications*, edited by Isaac Hernández-Calderón and René Asomoza, AIP Conf. Proc. No. 378 (AIP, Woodbury, NY, 1996), p. 619.
[5] N. Lorente and R. Monreal, Surf. Sci. **370**, 324 (1997).
[6] R. A. Baragiola and C. A. Dukes, Phys. Rev. Lett. **76**, 2547 (1996).
[7] R. A. Baragiola, S. M. Ritzau, R. C. Monreal, C. A. Dukes, and P. Riccardi, Nucl. Instrum. Methods Phys. Res. B **157**, 110 (1999); P. Riccardi, P. Barone, M. Camarca, A. Oliva, and R. A. Baragiola, *ibid.* **164-165**, 886 (2000); P. Barone, R. A. Baragiola, A. Bonanno, M. Camarca, A. Oliva, P. Riccardi, and F. Xu, Surf. Sci. **480**, L420 (2001); R. A. Baragiola, C. A. Dukes, and P. Riccardi, Nucl. Instrum. Methods Phys. Res. B **182**, 73 (2001).
[8] D. L. Mills, Surf. Sci. **294**, 161 (1993).
[9] H. Winter, Nucl. Instrum. Methods Phys. Res. B **78**, 38 (1993).
[10] T. Hecht, H. Winter, and A. G. Borisov, Surf. Sci. **406**, L607 (1998).
[11] H. Jouin, F. A. Gutierrez, and C. Harel, Phys. Rev. A **63**, 052901 (2001); **66**, 019901(E) (2002).
[12] N. Lorente, M. A. Cazalilla, J. P. Gauyacq, D. Teillet-Billy, and P. M. Echenique, Surf. Sci. **411**, L888 (1998).
[13] M. A. Cazalilla, N. Lorente, R. Diez-Muiño, J. P. Gauyacq, D. Teillet-Billy, and P. M. Echenique, Phys. Rev. B **58**, 13 991 (1998).
[14] J. Burgdorfer, E. Kupfer, and H. Gabriel, Phys. Rev. A **35**, 4963 (1987).
[15] J. Merino, *et al.*, Phys. Rev. B **57**, 1947 (1998).
[16] C. Denton, J. L. Gervasoni, R. O. Barrachina, and N. R. Arista, Phys. Rev. A **57**, 4498 (1998).
[17] K. D. Tsuei, E. W. Plummer, A. Liebsch, K. Kempa, and P. Bakshi, Phys. Rev. Lett. **64**, 44 (1990); K. D. Tsuei, E. W. Plummer, A. Liebsch, E. Pehlke, K. Kempa, and P. Bakshi, Surf. Sci. **247**, 302 (1991).
[18] P. J. Jennings, R. O. Jones, and H. Weinert, Phys. Rev. B **37**, 6113 (1988).
[19] F. A. Gutierrez, H. Jouin, S. Jequier, and M. Riquelme, Surf. Sci. **431**, 269 (1999).
[20] C. Bottcher, J. Phys. B **6**, 2368 (1973).
[21] H. Jouin, F. A. Gutierrez, and C. Harel, Surf. Sci. **417**, 18 (1998).
[22] D. S. Gemmel, Rev. Mod. Phys. **46**, 129 (1974).

[23] J. P. Ziegler, J. P. Biersack, and U. Littmark, *The Stopping and Range of Ions in Solids* (Pergamon, New York, 1985).

[24] M. Kato, R. S. Williams, and M. Aono, Nucl. Instrum. Methods Phys. Res. B **33**, 462 (1988).

[25] S. Jequier, H. Jouin, C. Harel, and F. A. Gutierrez, Nucl. Instrum. Methods Phys. Res. B **205**, 709 (2003).

[26] Under this circumstance it is clear that the (one-electron) tunnel resonant charge exchange mode is not relevant to our discussion while radiative transitions are known to have a negligible contribution to ion neutralization.

[27] If instead of a sheet of electrons we consider a semisphere of radius ρ immersed in the metal with its flat side on the surface, then the number $\tilde{N}$ of electrons around e^* is $\tilde{N} \simeq \frac{1}{2}[(\rho/r_s)^3 - 1]$. Taking $\rho = 2s$ for $s/r_s = (2,5,10)$ one gets approximately $\tilde{N} = (32,500,4000)$, which is noticeably larger than N. However, those electrons within the semisphere at a distance larger than $2r_s$ from the surface into the metal will be more likely related to volume plasmons than to surface plasmons.

[28] F. A. Gutierrez, C. Harel, S. Jequier, and H. Jouin, Nucl. Instrum. Methods Phys. Res. B **203**, 16 (2003).